

## Assessment of Natural Radioactivity and its Associated Hazards in Ras Hankorab Beach, South Marsa Alam City, Egypt

Manar A.M. Emam<sup>1</sup>, E. S. AbdEl-Halim<sup>1</sup>, M.A.M. Mahmoud<sup>2</sup>,  
Nadia Walley El-Dine<sup>1</sup>

<sup>1</sup> Faculty of women for Arts, Science and Education, Physics Department, Ain Shams University, Cairo, Egypt

<sup>2</sup> Nuclear Materials Authority, Cairo, Egypt

### ABSTRACT

Natural radiation levels of gamma ray emitted from  $^{238}\text{U}$ ,  $^{226}\text{Ra}$ ,  $^{232}\text{Th}$  and  $^{40}\text{K}$  in the beach sand of Ras Hankorab Area, South Marsa Alam City, Egypt have been carried out using the high purity germanium (HPGe) detector. Radiation hazard indices were calculated to estimate the radiological risk for the public and environment. The mean value of outdoor gamma absorbed dose rate ( $D_{out}$ ) for the studied areas is 62 nGy/h. Also the average value of annual outdoor effective dose ( $E_{out}$ ) for analyzed samples were measured and were lower than the acceptable values. The external radiation hazard indices were lower than unity for all samples. The outdoor excess life time cancer risk ( $ELCR_{out}$ ) and annual effective dose from radon ( $AED_{Rn}$ ) for all studied samples are lower than the allowed limits. The important minerals which are found in the studied area using XRD technique are: Ilmenite, Rutile, Magnetite, Ggothite, Garnet, zircon, Sphene, monazite, Uranothorite, Xenotime, and Apatite, as well as fine fragments of feldspars and quartz. Trace elements were analyzed by XRF technique. So the beach sand in Ras Hankorab area is safe and not pose any significant source of radiation hazard to the population and the tourists.

**Keywords:** Natural radionuclides - Beach sand - Hazard indices - HPGe

Date of Submission: 13-05-2020

Date of Acceptance: 25-05-2020

### I. Introduction

Radiation and radioactivity in the environment have natural and man-made sources(1). Exposure to natural radiation represents the most significant Part of the total exposure to radiation in the environment(2). Only natural radionuclides with half-lives comparable with the age of the earth or their corresponding decay products existing in terrestrial material are of great interest(3). The levels of these radionuclides are relatively distributed in soil based on the nature of its geological formation(4). The study of the activity of natural radionuclides in sands allows us to evaluate the radiological risk due to the external gamma radiation exposure for the population and tourists who spend their holidays in these beaches.

In this article, sand samples from the beach of Ras Hankorab along the coastline of Red sea were analyzed to determine the activity concentration of natural gamma-emitting radionuclides(5). The description of the climate in Ras Hankorab area can be summarized as follows: Ras Hankorab area is characterized by arid condition, hot climate, rainless in summer and sometimes with rains in winter. The area is important site because of their unique flora and fauna and therefore, they have been declared as natural protectorates(6). The diverse in geology and climate within the area provide favorable habitat for a wide variety of coastal and desert plants having valuable ecological benefits(7).

It is important to have knowledge about the natural background baseline of the radiological aspects so that potential environmental changes for the natural resources in future could be determined with a proper manner.

The main concern of this work is to study the environmental radiological aspects in the environment of Ras Hankorab area, the overall objectives are;

- 1- To determine the activity concentrations and distributions of gamma ray emitters radionuclides Ra-226, (U-238 series), (Th-232 series) and K-40 in sand.
- 2- To assess their possible associated hazards; The radiological obtain data and information from this study are highly needed to provide a basis for the sustainable development strategies(8).

### LOCATION

Ras Hankorab beach is covered nearly 3 km<sup>2</sup> and located on the Red sea coastal plain about 80 km south of Marsa Alam city. It is easily accessible through asphaltic Marsa Alam – Shalatin Highway (Fig.1). Wadi El Gemal-Ras Hankorab district is characterized by natural features which are tourist resources found at the Red sea

coast such as Wadi El Gemal Diving center, shams Alam tourist village and many archeological sites such as Sikait temple, Madinet Nugrus and ancient emerald mines at Um Addebaa, Um Kabu and Wadi Sikaitas well as Ras Hankorab beach. The main economic activities of inhabitants are tourism, herding (camel and sheep), fishing, mining works, goods trading and craft productions.

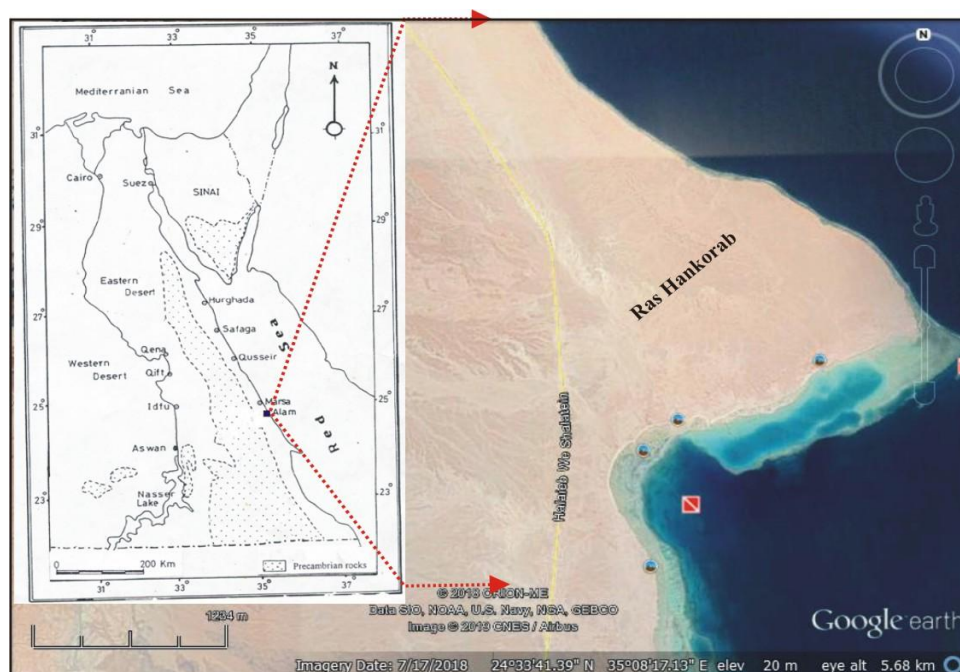


**Fig. (1): Location map of Ras Hankorab**

#### **SAMPLE COLLECTION AND PREPARATION**

Through 17 stations, 34 bulk samples were collected covering the beach of the Ras Hankorab area (Fig. 2). The studied samples were collected from digging boreholes using geological hammers, where each station contains two samples, one from the surface and the other from a depth of about 40 cm at the same point, with each sample weighing around 1 kg. After collection, each sample was air-dried for several days. The samples were ground, homogenized and sieved to about 200 mesh by a crushing machine. The bottles were completely sealed for more than one month to allow radioactive equilibrium to be reached. This step is necessary to ensure that radon gas is confined within the volume and the daughters will also remain in the sample. Then the samples were taken for gamma-spectrometric analysis, using a high purity germanium detector.

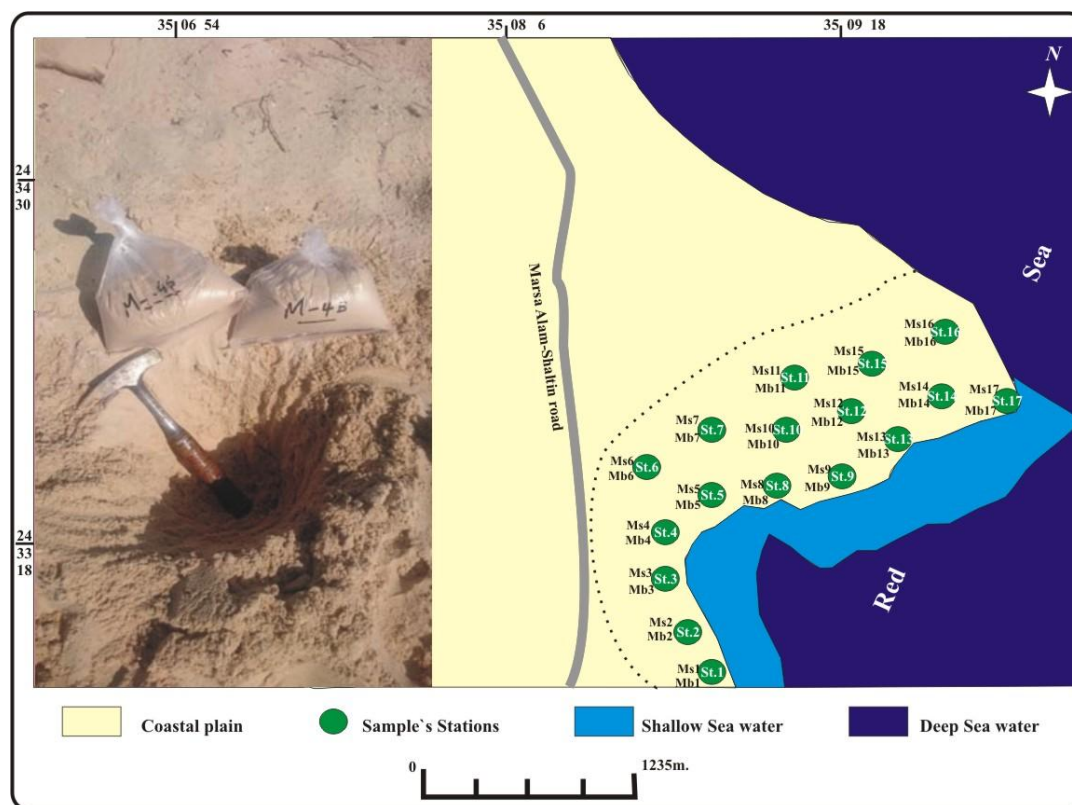


Fig. (2):Photograph and Samples location map at Ras Hankorab area

#### EXPERIMENTAL TECHNIQUE FOR HYPER PURE GERMANIUM

To estimate the activity levels of the  $^{238}\text{U}$ ,  $^{226}\text{Ra}$ ,  $^{232}\text{Th}$  and  $^{40}\text{K}$  in the studied samples, a high resolution gamma detection system in the laboratory of nuclear physics, faculty of women, Ain Shams University, was used for gamma analysis. The detection system is basically a hyper pure germanium (HPGe), model No. GEM-15190, coaxial type ORTEC, recommended operating bias, negative 3kV, with sensitive volume  $76.11\text{cm}^3$ . The energy resolution of HPGe detector was 1.9keV at 1332.5keV gamma ray line of  $^{60}\text{Co}$ . The quantitative analysis was achieved by using a maestro-H.E.G.&G card which was interfaced with IBM PC compatible to work as a multichannel analyzer (MCA). All the gamma measurements were taken after calibrating the MCA with  $\text{Co-60}$ ,  $\text{Am-241}$  and  $\text{Ra-226}$  point source.

The efficiency curve of the HPGe detector in the energy range from 186 keV to 2450 keV was obtained through two stages. In the first stage the relative efficiency curve of the detector was performed using a  $\text{Ra-226}$  point source (9). In the second stage, the average relative curve of the detector was normalized to an absolute efficiency curve for certain geometrical configuration and normalization factor for these geometries. Polyethylene bottles have been determined. For this purpose standard solution of potassium chloride has been used (10). The individual samples were placed on the detector manually during the work and each sample was counted for a time of 70000 seconds.

The gamma ray lines used to measure the activities of the studied isotopes are as follows (11);

For  $^{238}\text{U}$  was determined from the gamma rays emitted by its daughter products  $^{234}\text{Th}$  (63.3 keV) and  $^{234\text{m}}\text{Pa}$  (1001 keV),  $^{214}\text{Pb}$  from (351.9, 295.2) keV,  $^{214}\text{Bi}$  from (609.3, 1120.8, 1238.1 and 1764.8 keV), for  $^{226}\text{Ra}$  was measured using (186.2 keV) from its own gamma ray, for thorium series, the activity was measured from  $^{228}\text{Ac}$  (911.1, 968.9 keV) and  $^{208}\text{Tl}$  (583.1 keV) and  $^{40}\text{K}$  was measured using (1460.8 keV) (12). The detector was surrounded by a lead cylindrical shield to eliminate the contribution of naturally occurring background radionuclides in the environment. However, an empty bottle with the same geometry was measured for subtracting the background to have more accurate results (13).

#### Radioactivity counting

The net count after background corrections in each photo peak was used in the computation of activity concentration  $C$  (Bq/Kg) for each of the radionuclides in the samples using the expression (14).

$$C(\text{Bq Kg}^{-1}) = \frac{C_a}{I M \xi}$$

Where  $C_a$  the net count rate per second under each photo peak for each radionuclide,  $\xi$  the detector efficiency for the specific gamma ray,  $I$  is the reference intensity of the gamma line in a radionuclide and  $M$  is the mass of sample in (Kg).

### Radiation hazard indices

#### 1- radiation level index ( $I_{\bar{0}}$ )

This index can be used to estimate the level of gamma radiation hazard associated with the natural radionuclides in the samples. It is given by the equation;

$$I_{\bar{0}} = C_{Ra}/150 + C_{Th}/100 + C_K/1500$$

Where  $C_{Ra}$ ,  $C_{Th}$  and  $C_K$  are activity concentration of  $^{226}Ra$ ,  $^{232}Th$  and  $^{40}K$  in Bq/Kg respectively.

The value of this index must be less than unity in order to keep the radiation hazard insignificant (15).

#### 2- External hazard index ( $H_{ex}$ )

The external hazard index represents the external radiation exposure associated with gamma irradiation from radionuclides of concern. The value of  $H_{ex}$  should not exceed the maximum acceptable value of one in order to keep the hazard insignificant, the external hazard index is defined by the equation;

$$H_{ex} = C_{Ra}/370 + C_{Th}/259 + C_K/4810 \leq 1$$

Where  $C_{Ra}$ ,  $C_{Th}$  and  $C_K$  are concentration of radium, thorium and potassium respectively (15).

#### 3- Outdoor External Dose ( $D_{out}$ )

The absorbed gamma dose rates in air at 1m above the ground surface for the uniform distribution of radionuclides ( $^{238}U$ ,  $^{232}Th$  and  $^{40}K$ ) were calculated by the equation (16);

$$D_{out} = 0.427 C_U + 0.662 C_{Th} + 0.043 C_K \text{ (nGy/h)}$$

Where  $C_U$ ,  $C_{Th}$  and  $C_K$  are the activity concentration of uranium, thorium and potassium in Bq/Kg respectively.

#### 4- Annual outdoor effective dose $E_{out}$

The annual outdoor effective dose is estimated from the outdoor external dose rate  $D_{out}$ , time of stay in the outdoor or occupancy factor (of 20% of 8760 h in a year) and conversion factor ( $CF=0.7$  Sv/Gy) to convert the absorbed dose in air to effective dose. The  $E_{out}$  was calculated using the following equation (17);

$$E_{out} = D_{out} \text{ (nGy/h)} \times 0.2 \times 8760 \text{ h} \times 0.7 \text{ (Sv/Gy)}$$

#### 5- Outdoor Excess lifetime cancer risk (ELCR<sub>out</sub>)

Its value depends on value of annual outdoor effective dose. Thus, outdoor Excess lifetime cancer risk is calculated using the equation;

$$ELCR_{out} = E_{out} \times LE \times RF$$

Where  $E_{out}$  is annual outdoor effective dose,  $LE$  life expectancy (66 years) and  $RF$  ( $Sv^{-1}$ ) is risk factor per Sievert, which is 0.05 (18).

#### 6- Radon estimation

Firstly, the radon mass exhalation rate  $E_{Rn}$  depends on emanation factor  $F_{Rn}$  which depends on activity concentration of radon  $C_{Rn}$ .

The activity concentration of radon  $C_{Rn}$  is calculated from through  $C_{Ra}$  activity concentration of radium  $^{226}Ra$  in Bq/Kg and  $C_D$  activity concentration of one of daughters of radium lead  $^{214}Pb$  or bismuth  $^{214}Bi$  in Bq/Kg

$$C_{Rn} = (C_{Ra} - C_D) \times p \text{ (Bq/m}^3\text{)}$$

Where  $p$  is density of radon (9.73 Kg/m<sup>3</sup>)

The radon exhalation rate is calculated using the equation;

$$E_{Rn} = F_{Rn} \times C_{Ra} \times \lambda_{Rn} \text{ (Bq/Kg.S)}$$

Where  $F_{Rn}$  is emanation factor and is calculated from the equation;

$$F_{Rn} = (C_{Ra} - C_D) / C_{Ra}$$

And  $\lambda_{Rn}$  is decay constant of  $^{222}Rn$  ( $2.1 \times 10^{-6} S^{-1}$ ).

Secondly, the annual effective dose  $AED_{Rn}$  in (mSv/y) is calculated by using the equation

$$AED_{Rn} = \frac{C_{Rn} \times 0.4 \times K \times H}{3700 \text{ (Bq m}^{-3}\text{)} \times 170 \text{ h}}$$

Where  $C_{Rn}$  is activity concentration of radon ( $Bq/m^3$ ), K is the ICRP dose conversion factor ( $5mSv WLM^{-1}$  for occupational workers) and H is the annual occupancy at the location (2160 h for workers)(19). And 170h is exposure hours taken for  $WLM^{-1}$ .

## II. Result And Discussion

Activity concentrations of  $^{238}U$ ,  $^{226}Ra$ ,  $^{232}Th$  and  $^{40}K$  for the studied sand samples of Ras Hankorab beach surface are given in table (1). The average activity concentrations are 116.1, 113.8, 7.7 and 181.2  $Bq/Kg$  for  $^{238}U$ ,  $^{226}Ra$ ,  $^{232}Th$  and  $^{40}K$  respectively. The activity concentrations of all studied samples for uranium and radium are higher than the permissible level, but the activity concentrations of all studied samples for thorium and potassium are lower than the permissible level as shown in figure (3). The radioelements permissible level values are 33  $Bq/Kg$  for  $^{238}U$ , 32  $Bq/Kg$  for  $^{226}Ra$ , 45  $Bq/Kg$  for  $^{232}Th$  and 412  $Bq/kg$  for  $^{40}K$  (20). Also the activity concentrations of  $^{238}U$ ,  $^{226}Ra$ ,  $^{232}Th$  and  $^{40}K$  for the studied sand samples at the bottom were calculated as illustrated in table (2). The average activity concentrations are found to be 113.4, 117.8, 7.9 and 181.5  $Bq/Kg$ . The concentrations of  $^{238}U$  and  $^{226}Ra$  are higher than the permissible level, while the concentrations of  $^{232}Th$  and  $^{40}K$  are lower than the permissible level as shown in figure (4). The concentrations of  $^{238}U$ ,  $^{226}Ra$ ,  $^{232}Th$  and  $^{40}K$  on the surface and at the bottom samples are the same. The activity ratios  $^{226}Ra/^{238}U$  were calculated for all studied sand samples (table 1,2) which are for surface samples in range from (0.4-1.3) and for bottom samples (0.8-1.3). Samples in the bottom have a state of equilibrium more than that in the surface.

The concentrations of  $^{238}U$  and  $^{232}Th$  of the studied sand samples in ppm and activity ratio  $^{232}Th/^{238}U$  were calculated and illustrated in (table 3) for surface and bottom samples. The ratio  $^{232}Th/^{238}U$  for surface samples range between (0.12-0.29) and for bottom samples range between (0.11-0.29) which are lower than Clark's value (3.5) which indicate uranium enrichment.

**Table(1): Activity concentrations of  $^{238}U$ ,  $^{226}Ra$ ,  $^{232}Th$  and  $^{40}K$  in  $Bq/Kg$  and  $^{226}Ra/^{238}U$  ratio for the studied sand samples on the surface at Ras Hankorab beach.**

Samples	U-238	Ra-226	Th-232	K-40	$^{226}Ra/^{238}U$
M-1S	72.9	75.9	4.0	174.7	1.0
M-2S	116.6	131.8	8.6	216.9	1.1
M-3S	136.6	120.1	8.8	208.4	0.9
M-4S	94.5	115.7	5.8	159.1	1.2
M-5S	112.4	139.2	9.6	204.7	1.2
M-6S	41.9*	17.1*	1.8*	55.7*	0.4*
M-7S	205.0**	143.0**	8.3	171.0	0.7
M-8S	69.2	61.7	3.8	118.1	0.9
M-9S	165.6	133.5	9.0	167.2	0.8
M-10S	125.8	126.2	8.3	174.5	1.0
M-11S	99.6	113.2	9.6	162.4	1.1
M-12S	101.6	134.7	8.2	146.2	1.3**
M-13S	106.7	105.7	9.1	264.4**	1.0
M-14S	116.3	124.0	8.5	206.8	1.1
M-15S	116.3	135.6	8.6	187.7	1.2
M-16S	126.4	127.3	10.1**	240.7	1.0
M-17S	166.0	130.6	8.0	221.4	0.8
Average	116.1	113.8	7.7	181.2	1.0

\*lower value, \*\*higher value

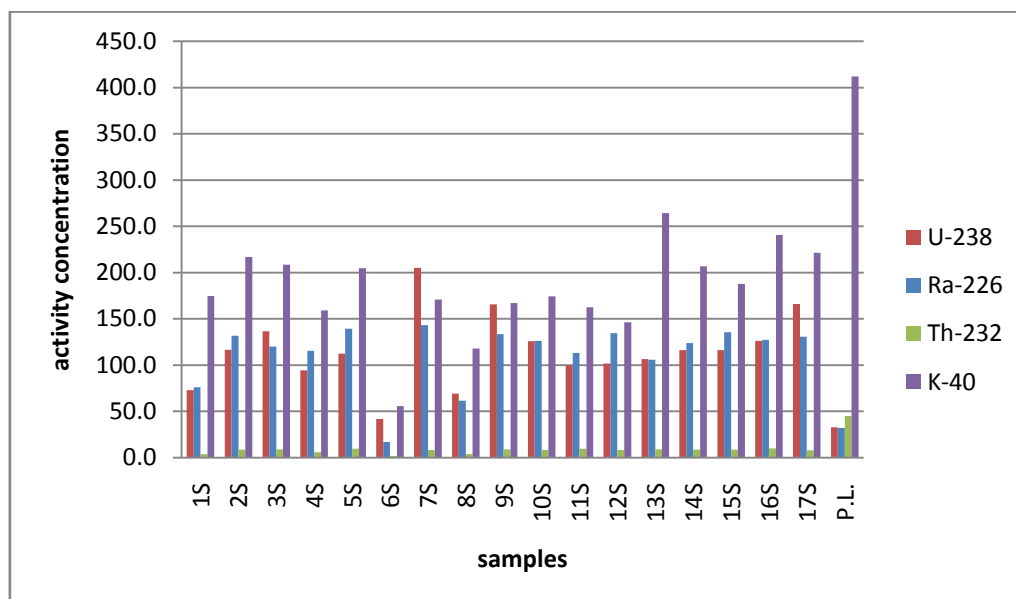


Fig.(3):Activity concentrations of <sup>238</sup>U, <sup>226</sup>Ra, <sup>232</sup>Th and <sup>40</sup>K for surface samples with permissible level.

Table (2): Activity concentrations of <sup>238</sup>U, <sup>226</sup>Ra, <sup>232</sup>Th and <sup>40</sup>K in Bq/Kg and <sup>226</sup>Ra/<sup>238</sup>U ratio for the studied sand samples at the bottom at Ras Hankorab beach.

Samples	U-238	Ra-226	Th-232	K-40	<sup>226</sup> Ra/ <sup>238</sup> U
M-1B	93.9	112.0	5.7	236.8	1.2
M-2B	116.6	128.5	9.7	174.3	1.1
M-3B	44.1*	56.4*	3.1*	112.3*	1.3**
M-4B	157.0	144.2	8.0	192.6	0.9
M-5B	103.6	90.3	7.9	149.4	0.9
M-6B	121.0	145.7**	8.7	177.0	1.2
M-7B	120.8	139.0	8.1	163.2	1.2
M-8B	107.3	117.2	5.4	136.9	1.1
M-9B	139.6	139.4	4.9	161.6	1.0
M-10B	113.6	105.4	5.6	161.8	0.9
M-11B	164.0**	136.1	10.8	199.8	0.8*
M-12B	117.4	136.1	11.1**	165.8	1.2
M-13B	92.6	92.0	8.3	186.8	1.0
M-14B	118.1	131.2	9.3	227.6	1.1
M-15B	88.9	99.4	8.6	165.0	1.1
M-16B	118.6	108.5	10.2	255.7**	0.9
M-17B	110.6	122.0	9.1	219.7	1.1
average	113.4	117.8	7.9	181.5	1.1

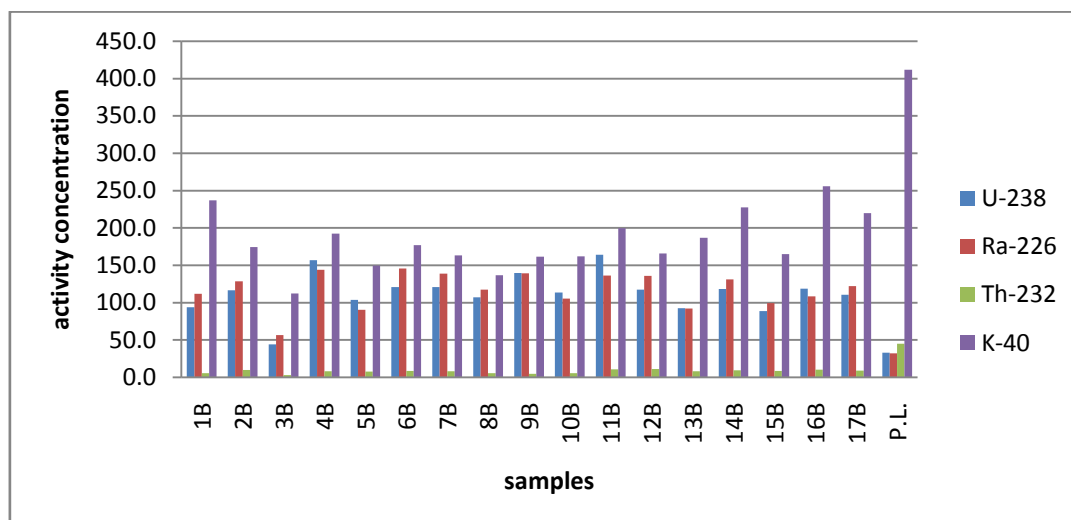


Fig.(4):Activity concentrations of <sup>238</sup>U, <sup>226</sup>Ra, <sup>232</sup>Th and <sup>40</sup>K for bottom samples with permissible level.

Table(3):<sup>238</sup>U and <sup>232</sup>Th concentration in sand samples in ppm and <sup>232</sup>Th/<sup>238</sup>U ratio for surface and bottom samples.

Surface samples.				Bottom samples.			
Samples	U-238	Th-232	<sup>232</sup> Th/ <sup>238</sup> U	Samples	U-238	Th-232	<sup>232</sup> Th/ <sup>238</sup> U
M-1S	5.90	0.97	0.16	M-1B	7.60	1.41	0.19
M-2S	9.44	2.13	0.23	M-2B	9.44	2.38	0.25
M-3S	11.06	2.18	0.20	M-3B	3.57	0.77	0.21
M-4S	7.65	1.43	0.19	M-4B	12.71	1.97	0.15
M-5S	9.10	2.35	0.26	M-5B	8.39	1.94	0.23
M-6S	3.39	0.45	0.13	M-6B	9.80	2.13	0.22
M-7S	16.60	2.05	0.12	M-7B	9.78	2.00	0.20
M-8S	5.61	0.94	0.17	M-8B	8.69	1.33	0.15
M-9S	13.41	2.21	0.17	M-9B	11.30	1.20	0.11
M-10S	10.19	2.04	0.20	M-10B	9.20	1.38	0.15
M-11S	8.07	2.38	0.29	M-11B	13.28	2.66	0.20
M-12S	8.23	2.03	0.25	M-12B	9.50	2.72	0.29
M-13S	8.64	2.24	0.26	M-13B	7.50	2.06	0.23
M-14S	9.42	2.09	0.22	M-14B	9.56	2.30	0.22
M-15S	9.41	2.11	0.22	M-15B	7.20	2.12	0.20
M-16S	10.24	2.49	0.24	M-16B	9.60	2.51	0.15
M-17S	13.44	1.96	0.15	M-17B	8.96	2.25	0.11

The gamma ray radiation hazards due to the specified radionuclides were assessed by radiological parameters such as indices; outdoor external dose (nGy/h), external hazard,annual outdoor effective dose (mSv/y) and outdoor excess life time cancer risk at surface and bottom sand beach samples as shown in (table 4). We concluded that the outdoor external dose rate ranged between (21.5-100.4) for surface and ranged between (25.7-85.8) in bottom with an average value 62.4 and 61.5 nGy/h respectively which are slightly higher than permissible level (59 nGy/h) (21).

Table (4):The values of external hazard (H<sub>ex</sub>),outdoor external dose rate (D<sub>out</sub>) in nGy/h,annual outdoor effective dose rate (mSv/y) and outdoor Excess life time cancer risk (ELCR<sub>out</sub>)at surface and bottom beach sand samples.

		H <sub>ex</sub>	D <sub>out</sub> (nGy/h)	E <sub>out</sub> (mSv/Y)	ELCR <sub>out</sub> x10 <sup>-3</sup>
M-1	Surface	0.3	41.2	0.05	0.17
	Bottom	0.37	54.06	0.07	0.22
M-2	Surface	0.4	64.8	0.08	0.26
	Bottom	0.42	63.70	0.08	0.26
M-3	Surface	0.4	73.1	0.09	0.30
	Bottom	0.19	25.70	0.03	0.10
M-4	Surface	0.4	51.0	0.06	0.21
	Bottom	0.46	80.60	0.10	0.33
M-5	Surface	0.5	63.1	0.08	0.26
	Bottom	0.31	55.87	0.07	0.23
	Surface	0.1	21.5	0.03	0.09

M-6	Bottom	0.46	65.01	0.08	0.26
M-7	Surface	0.5	100.4	0.12	0.41
	Bottom	0.44	63.97	0.08	0.26
M-8	Surface	0.2	37.2	0.05	0.15
	Bottom	0.37	55.29	0.07	0.22
M-9	Surface	0.4	83.8	0.10	0.34
	Bottom	0.43	69.76	0.09	0.28
M-10	Surface	0.4	66.7	0.08	0.27
	Bottom	0.34	59.19	0.07	0.24
M-11	Surface	0.4	55.9	0.07	0.23
	Bottom	0.45	85.77	0.11	0.35
M-12	Surface	0.4	55.1	0.07	0.22
	Bottom	0.44	64.57	0.08	0.26
M-13	Surface	0.4	63.0	0.08	0.25
	Bottom	0.32	53.08	0.07	0.21
M-14	Surface	0.4	64.2	0.08	0.26
	Bottom	0.44	66.39	0.08	0.27
M-15	Surface	0.4	63.4	0.08	0.26
	Bottom	0.34	50.73	0.06	0.21
M-16	Surface	0.4	71.0	0.09	0.29
	Bottom	0.39	68.38	0.08	0.28
M-17	Surface	0.4	85.7	0.11	0.35
	Bottom	0.41	62.75	0.08	0.25

The results show that the average values of the annual outdoor effective dose  $E_{out}$  for surface and bottom samples equal 0.08 which is slightly higher than permissible value 0.07 mSv/y(22). The average value of  $ELCR_{out}$  equal  $(0.25 \times 10^{-3})$  for surface and bottom samples and less than permissible value  $(0.29 \times 10^{-3})$ . So the sand beach of the area under investigation is not dangerous on people and can be used as a tourist beach. Tables(5) represent the activity concentration of radon  $C_{Rn}$ , radon emanation factor F, radon mass exhalation rate  $E_{Rn}$  and the annual effective dose from radon  $AED_{Rn}$  for surface and bottom samples.

**Table (5): The values of activity concentrations of radon  $^{222}Rn$  (Bq/m<sup>3</sup>), radon emanation factor (F), radon mass exhalation rate ( $E_{Rn}$ ) and annual effective dose from radon ( $AED_{Rn}$ ) for the surface and bottom beach sand samples.**

		$C_{Rn}$ (Bq/m <sup>3</sup> )	F	$E_{Rn}$ (mBq/Kg.s)	$AED_{Rn}$ (msv/y)
M-1	Surface	500.1	0.68	0.11	3.43
	Bottom	857.93	0.79	0.19	5.89
M-2	Surface	1023.4	0.80	0.22	7.03
	Bottom	1030.25	0.82	0.22	7.08
M-3	Surface	890.0	0.76	0.19	6.11
	Bottom	389.27	0.71	0.08	2.67
M-4	Surface	911.1	0.81	0.20	6.26
	Bottom	1137.69	0.81	0.25	7.81
M-5	Surface	1087.6	0.80	0.23	7.47
	Bottom	647.61	0.74	0.14	4.45
M-6	Surface	67.1	0.40	0.01	0.46
	Bottom	1128.32	0.80	0.24	7.75
M-7	Surface	1146.2	0.82	0.25	7.87
	Bottom	1134.39	0.84	0.24	7.79
M-8	Surface	436.9	0.73	0.09	3.00
	Bottom	908.20	0.80	0.20	6.24
M-9	Surface	1015.4	0.78	0.22	6.97
	Bottom	1081.40	0.80	0.23	7.43
M-10	Surface	960.7	0.78	0.21	6.60
	Bottom	791.64	0.77	0.17	5.44
M-11	Surface	837.5	0.76	0.18	5.75
	Bottom	993.10	0.75	0.21	6.82
M-12	Surface	1049.2	0.80	0.23	7.21
	Bottom	1048.18	0.79	0.23	7.20
M-13	Surface	717.0	0.70	0.15	4.92
	Bottom	653.25	0.73	0.14	4.49
M-14	Surface	892.9	0.74	0.19	6.13
	Bottom	1037.33	0.81	0.22	7.12
M-15	Surface	1041.7	0.79	0.22	7.15
	Bottom	789.30	0.82	0.17	5.42
M-16	Surface	974.7	0.79	0.21	6.69
	Bottom	756.72	0.72	0.16	5.20
	Surface	951.9	0.75	0.21	6.54



M-17	Bottom	883.56	0.74	0.19	6.07
------	--------	--------	------	------	------

The Activity concentration of <sup>222</sup>Rn were varied between (67.1 -1146.2) Bq/m<sup>3</sup> for surface samples and between (389.3-1137.7)Bq/m<sup>3</sup> for bottom samples. The values of the radon emanation factor F and the radon mass exhalation rate for surface samples are ranged from (0.4-0.82) and (0.01-0.25) mBq/Kg.s while for bottom samples are ranged from (0.71-0.84) and (0.08-0.25)mBq/Kg.s respectively. The annual effective dose from radon AED<sub>Rn</sub> ranged between (0.46-7.87) and (2.67-7.81) mSv/y for surface and bottom samples respectively. The results indicate low levels of annual effective dose from radon in sand beach. All the samples in this location were lower than the maximum permissible dose limits (10mSv/y) recommended by ICRP(23).

### III. Geochemistry

Each two collected bulk samples from surface and bottom at each station was mixed to be 17 samples and soaked in water and treated with a mixture of stannous chloride and hydrochloric acid to cleaning of the grains from any coating of carbonates or oxides, or even oxyhydroxides.

The samples were subject to heavy minerals separation using the bromoform liquid to separate the heavy minerals fraction from the light mineral fraction. The obtained data and the attached histogram are listed in (table 6).

Using XRD technique we have shown that samples consist of light and heavy constituents, but the light mineral constituents are feldspar, quartz, and lithic fragments, while the heavy minerals contain Ilmenite, Rutile, Magnetite, Ggoethite, Garnet, zircon, Sphene, monazite, Uranothorite, Xenotime, and Apatite. The heavy minerals reflect the nature of source rock area because different rock types contain different heavy mineral associations.

**Table (6): Percentages of light and heavy minerals of the studied samples with histogram attached, of the studied sand beach at Ras Hankorab, Southeastern Desert.**

St.no.	Light %	Heavy %
M1	95.4	5.2
M 2	94.6	5.5
M 3	95.0	5.4
M 4	92.1	7.2
M 5	92.9	7.9
M 6	93.9	6.2
M 7	96.2	3.1
M 8	96.8	3.0
M 9	94.0	3.3
M 10	90.9	4.9
M 11	91.7	5.5
M 12	95.2	7.3
M 13	95.3	4.9
M 14	94.7	8.2
M 15	93.8	9.2
M 16	92.9	4.7
M 17	95.0	5.7

The identified important minerals in the studied samples at Ras Hankorab beach which they are confirmed by the XRD technique and seen by the binocular microscope are as follow;

**Ilmenite (FeTiO<sub>3</sub>)** represents the major mineral constituent of the total mineral assemblages of the studied very fine sand samples.

**Rutile (TiO<sub>2</sub>)** occurs as euhedral tetragonal prisms with rounded pyramidal terminations, constitutes about 0.25 wt% of the original raw sand (reaching 3 % of the total minerals of Ras Hankorab beach sands).

**Magnetite (Fe<sub>3</sub>O<sub>4</sub>)** is a second abundant mineral constitutes about 15% of the total minerals. **Goethite FeO(OH)** is a reddish and brownish black in colour and formed due to the disintegration of pyrite (FeS<sub>2</sub>). It is exist in the all studied samples.

**Garnet [X<sub>3</sub>Y<sub>2</sub>(SiO<sub>4</sub>)<sup>3</sup>]** forms about 11% of the total heavy minerals with 0.95 wt%. It characterized by vitreous luster garnet grains reflect pink to brownish red color occasionally with a violet tint and occur as euhedral crystals, sharp irregular fragments, and sub-rounded to rounded grains.

**Zircon** ( $ZrSiO_4$ ) crystals are colorless with internal shades of reddish brown color probably due to iron oxide stains. Another zircon variety that reflect orange, rosy, brown and deep red color grains, besides, metamictic and zoned zircon grains occur as brittle or fractured crystals that probably due to radioactive decay.

**Sphene (titanite)** [ $CaTi [SiO_4] (O, OH, F)$ ] exhibit the lowest abundant content (3%) of the total minerals.

**Monazite** [(LREE, Th)  $PO_4$ ] occurs as brown to reddish brown prismatic crystals or even tabular habit. Thorium is usually exists in monazite in substitution for the REE.

**Uranothorite** (U,Th,Y)  $SiO_4$  is a dark brown grains with a resinous or greasy luster and it is non-magnetic but recovered from the weakly magnetic fraction due to its iron content.

**Xenotime** (Y, HREE)  $PO_4$  occurs as pink to red grains, with a resinous luster. It was recovered in the moderately magnetic fraction.

**Apatite**  $\{Ca_4(Ca,F,Cl,OH)(PO_4)^3\}$  exists as a minor constituent, colorless to pale yellow, transparent, and rounded grains.

The analysis has shown that the beach sand of Ras Hankorab contain a thin layers of black sand, where there are a small concentration of heavy minerals such as monazite and zircon, so that it can be used as therapy.

### X-Ray Fluorescence

In this study the trace elements were analyzed by XRF technique for 17 samples to know the dominant trace elements at Ras Hankorab sand beach. Concentration of Eleven trace elements (Cr, Ni, Cu, Zr, Rb, Y, Ba, Pb, Sr, V and Nb) have been determined. The analyzed trace elements are listed in table (7).

**Table 7: Chemical analysis of some trace elements for the 17 samples of Ras Hankorab area with Pie-Chart showing the average distribution of analyzed trace elements.**

S.No.	Cr	Ni	Cu	Zr	Rb	Y	Ba	Pb	Sr	V	Nb
M1	28	15	61	101	179	19	69	65	8	22	6
M 2	25	11	82	116	220	13	79	71	11	30	7
M 3	28	13	75	125	166	11	82	59	10	32	5
M 4	23	20	76	124	191	13	75	62	10	33	6
M 5	30	13	80	111	168	15	84	49	12	38	6
M 6	31	18	80	88	170	17	58	45	9	22	4
M 7	37	16	81	130	172	13	109	55	12	36	5
M 8	32	14	81	132	166	10	87	30	10	37	6
M 9	30	15	80	145	89	16	119	29	12	36	9
M 10	40	19	76	141	177	12	79	33	12	37	7
M 11	27	16	66	100	171	10	58	56	8	25	4
M 12	35	15	85	126	206	13	92	60	11	31	7
M 13	22	19	66	123	146	11	84	48	9	36	6
M 14	19	20	59	130	180	14	79	52	10	37	4
M 15	26	17	60	131	188	13	89	29	10	28	5
M 16	24	18	72	98	160	15	68	30	8	22	4
M 17	35	16	73	110	152	13	109	39	9	26	6
Min.	19	11	59	88	89	10	58	29	8	22	4
Max.	40	20	85	145	220	19	119	71	12	38	9
Aver.	29.8	16.9	73.3	121.2	164.8	13.1	85.9	42.2	10	31.1	5.6

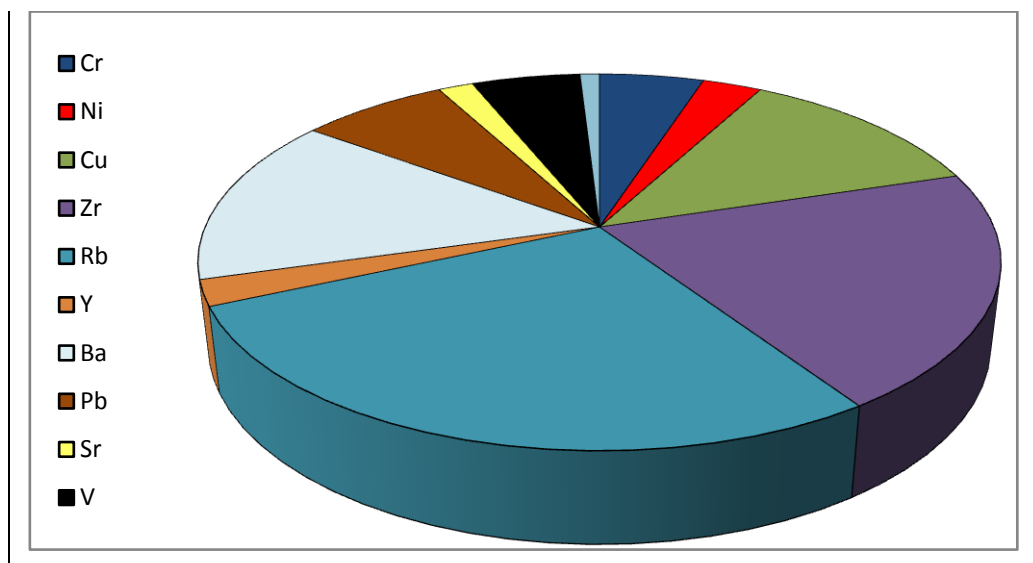


Fig.5 Pie-Chart showing the average distribution of analyzed trace elements.

It is clear that all samples contain high concentration of Rb, Zr, Ba, Cu and lead which can be separated using different methods to be used in different important industries.

#### IV. Conclusion

Specific activities distribution of natural radionuclide gamma ray activities which produced by  $^{238}\text{U}$ ,  $^{226}\text{Ra}$ ,  $^{232}\text{Th}$  and  $^{40}\text{K}$  were determined in 17 sand samples from the surface and 17 sand samples from the bottom at the same stations, which measured along Ras Hankorab area beach, using gamma-ray spectrometry. The measured studied samples showed higher radioactivity levels of  $^{238}\text{U}$  and  $^{226}\text{Ra}$  than the permissible level, while the concentrations of  $^{232}\text{Th}$  and  $^{40}\text{K}$  are lower than permissible level.

The concentrations of  $^{238}\text{U}$  and  $^{226}\text{Ra}$  in surface and bottom samples are nearly equal. The permissible level of  $E_{\text{out}}$  and  $\text{ELCR}_{\text{out}}$  were found to be within the allowed limits.

Physical separation of some important minerals in the studied area using XRD technique indicate that the sands of Ras Hankorab beach contain a thin layers of black sand, where there are a small concentration of heavy minerals such as monazite and zircon, so the beach can be suitable for therapy and medical treatments.

Concentration of Eleven trace elements (Cr, Ni, Cu, Zr, Rb, Y, Ba, Pb, Sr, V and Nb) using XRF technique have been determined, which can be separated using different methods to be used in different important industries.

**From this study the radiological impacts of radionuclides in the beach sand are negligible and it is safe, the sand not pose any significant source of radiation hazard to the population. So public and tourists can going to the beach for recreation or to the sailors and fishermen involved in their activities in the area under investigation.**

#### Reference

- [1]. Saleh, I.H., 2012. Radioactivity of  $^{238}\text{U}$ ,  $^{232}\text{Th}$ ,  $^{40}\text{K}$ , and  $^{137}\text{Cs}$  and assessment of depleted uranium in soil of the Musandam Peninsula, Sultanate of Oman. Turkish J. Eng. Environ. Sci. 36, 236–248.
- [2]. UNSCEAR, 2008. United Nations Scientific Committee on the Effects of Atomic Radiation. Report to the General Assembly United Nations, New York. Annex B, vol. I, 223–439.
- [3]. Al-Jundi, J., Al-Bataina, B.A., Abu-Rukah, Y., Shehadeh, H.M., 2003. Natural radioactivity concentrations in soil samples along the Amman Aqaba Highway, Jordan. Radiat. Measur. 36, 555–560.
- [4]. Orabi, H., Al-Shareif, A., El Galefi, M., 2006. Gamma-ray measurements of naturally occurring radioactive sample from Alkharje city. J. Radioanal. Nucl. Chem. 269, 99–102.
- [5]. BahaEl Din, S.M. (2001). Important bird areas in Africa and associated islands – Egypt, available online: <http://www.birdlife.org>, pp.241-264.
- [6]. FAO, 2002. Rehabilitation, conservation and sustainable utilization of mangroves in Egypt, Community-based mangrove rehabilitation and ecotourism development and management in the Red Sea coast, Consultancy Report, TCP/EGY/0168(A), p71.
- [7]. IRG (International Resources Group for USAID) and EEAA Egyptian Environmental Affairs Agency Management plan for wadi El-Gemal National Park: Egyptian environmental Affairs Agency Nature Conservation Sector, Egypt Environmental Policy Program (EPPP), (2004), p.176.
- [8]. Arafat, A. A., et al., "Distribution of natural radionuclides and assessment of the associated hazards in the environment of Marsa Alam-Shalateen area, Red Sea coast, Egypt.", Journal of radiation research and applied sciences 10.3, (2017): 219-232.

- [9]. El-Tahawy, M. S., Farouk, M. A., Hammad, H. F., and Ibrahim, N. M., "Natural Potassium as A standard source for the Absolute Efficiency Calib. of Ge Detector", Nucl.Sci.J.29, p. (361), (1992).
- [10]. EML., "Environmental Measurements Laboratory USA", Department of Energy, Nov. (1990).
- [11]. Beretka, J., Mathew, P. J., "Natural radioactivity of Australian building materials, industrial wastes and byproducts", Health Physics 48, pp: 87–95., (1985).
- [12]. Merdanoğlu, M., and Altınsoy, N., "Radioactivity concentrations and dose assessment for soil samples from Kestanol granite area", Turkey. Radiation Protection Dosimetry 121 (No. 4), Dosimetry 125 (1–4), pp: 444–448., (2006).
- [13]. Ibrahim, M. E., et al., "Assessment of the Natural Radioactivity and its Radiological Hazards in Stream Sediments at Gulf of Al Aqaba, Sinai, Egypt." Journal of Scientific Research in Science 32, part 2 (2015): 62-75.
- [14]. UNSCEAR. United Nations Scientific Committee on the Effects of Atomic Radiation (2000), Sources and effects of ionizing radiation. Report V. 1 to General Assembly, with Scientific Annexes (NY), (2000).
- [15]. Bassioni G, Abdulla F, Morsy Z and El-Faramawy N., (2012). "Evaluation of Naturally Occurring Radioactive Materials (NORM) in Inorganic and Organic Oilfield Scales from the Middle East". Archives of Environmental Contamination and Toxicology. Volume 62, Issue 3, pp361-368.
- [16]. United Nations Scientific Committee on the Effects of Atomic Radiation, UNSCEAR, Sources and Effects of Ionizing Radiation, United Nations, New York, 1988.
- [17]. Abdullah Alamoudi, (2010). "The effect of grain size on the measurements of activity concentration of naturally occurring radioactive materials ". Department of Phy., Faculty of engineering and physical sciences university of surrey, (Mphil to PhD Transfer Report). pp.16-17.
- [18]. Qureshi A.A., Tariq S., Ud Din K., Manzoor S., Calligaris C. and Abdul Waheed., (2014). "Evaluation of excessive lifetime cancer risk due to natural radioactivity in the rivers sediments of Northern Pakistan ", Journal of Radiation Research and Applied Sciences, Issue 7, pp438-447.
- [19]. Nikl I and Vegvari L., (1992). "The natural radioactivity of coal and byproducts in Hungarian coal fired power plants". Izotop Technika Diagnosztika; V.35, PP.57-64.
- [20]. UNSCEAR, 2000. United Nations Scientific Committee on the Effects of Atomic Radiation Sources and Effects of Ionizing Radiation. United Nations Publication
- [21]. UNSCEAR, United Nations Scientific Committee on the Effect of Atomic Radiation, (2010). "Sources and Effects of Ionizing Radiation". Report to General Assembly with Scientific Annexes, United Nations, New York.
- [22]. UNSCEAR, (2008). Report to the general assembly. Annex B Exposure of the Public and workers from various sources of radiation.
- [23]. ICRP, International Commission on Radiological Protection, (1993). "Protection against radon-222 at home and at work". ICRP Publication No.65. Oxford: Oxford Pergamon Press.

Manar A.M. Emam, et. al. "Assessment of Natural Radioactivity and its Associated Hazards in Ras HankorabBeach, South Marsa Alam City, Egypt." *IOSR Journal of Applied Physics (IOSR-JAP)*, 12(3), 2020, pp. 41-52.